Atmos. Chem. Phys. Discuss., doi:10.5194/acp-2017-156, 2017
Manuscript under review for journal Atmos. Chem. Phys.
Discussion started: 1 March 2017

Observations of Particles at their Formation Sizes in Beijing, China

Rohan Jayaratne[1†], Buddhi Pushpawela[1†], Congrong He[1], Jian Gao[2], Li Hui[2], Lidia Morawska[1*],

1 International Laboratory for Air Quality and Health, Queensland University of Technology, GPO Box 2434, Brisbane 4001, Australia.
2 Chinese Research Academy of Environmental Sciences, Beijing 100012, China.

† Joint first authors.

* Corresponding author contact details:

Tel: (617) 3138 2616; Fax: (617) 3138 9079

Email: l.morawska@qut.edu.au

Abstract

New particle formation (NPF) has been observed in many highly polluted environments of South-East Asia, including Beijing, where the extent of its contribution to intense haze events is still an open question. Estimated characteristics of NPF events, such as their starting times and formation and growth rates of particles, are very different when the measurements are restricted to particles in larger size ranges. In order to understand the very first steps of particle formation, we used a neutral cluster and air ion spectrometer (NAIS) to investigate particle characteristics at sizes exactly where atmospheric nucleation and cluster activity occurs. Observations over a continuous three-month period in Beijing showed 26 NPF events. These events generally coincided with periods with relatively clean air when the wind direction was from the less-industrialized north. No NPF were observed when the daily mean $PM_{2.5}$ concentration exceeded 43 µg m^{-3}, which was the upper threshold for particle formation in Beijing. The fraction of particles that are charged in the size range 2-42 nm was normally about 15%. However, this fraction increased to 20-30% during haze events and decreased to below 10% during NPF events. With the NAIS, we determined the starting times of NPF very precisely to a greater accuracy than has been possible in Beijing before and provided a temporal distribution of NPF events with a maximum at about 8.30 am. Particle formation rates varied between 10-36 cm^{-3} s^{-1}. Particle growth rates were estimated to be in the range 0.5-9.0 nm h^{-1}. These results are more reliable than previous studies in Beijing as the measurements were conducted for the first time at the exact sizes where clusters form into particles and provide useful insight into the formation of haze events.

Keywords: New particle formation, secondary particles, nucleation, haze events

---

1. Introduction

Particles in the atmosphere may be classified into two types depending on their origin. Primary particles are directly emitted by a source while secondary particles are formed through a secondary process by the homogeneous condensation of gaseous precursors. This is known as new particle formation (NPF) and has been observed in many parts of the world in many different types of environment (Curtius, 2006;Kulmala et al., 2005;Kulmala et al., 2004;Zhang et al., 2011). NPF is a complicated process where molecular clusters come together to form particles at a size of about 1.6 nm (Kulmala et al., 2004). Generally, it is favoured by clean air conditions where the particle number concentration (PNC) in the atmosphere is low, resulting in a lower particle surface available for the condensation of gases, leading to an increase of the supersaturation in the air enhancing homogeneous condensation of the gaseous species (Kulmala et al., 2005;Wu et al., 2011) and, therefore, NPF is less frequent in polluted environments. However, if the gaseous precursor concentration is high enough, NPF may occur at even higher particle concentrations (Kulmala et al., 2005;Wu et al., 2011). Jayaratne et al. (2015) showed that in the relatively clean environment of Brisbane, Australia, NPF do not occur when the ambient PM_{10} concentration exceeds about 20 µg m^{-3}. However, NPF have been commonly observed in more polluted environments like Beijing (Kulmama et al., 2016) and Shanghai (Xiao et al., 2015) in China. The study of the formation and characteristics of NPF events in Beijing is important because of its possible influence on severe haze episodes (Guo et al., 2014;Huang et al., 2014). Such haze events not only give rise to poor visibility but are responsible for sharp increases in respiratory problems amongst the large population that is exposed. In particular, Beijing experienced severe haze episodes during November and December, 2015. Daily maximum $PM_{2.5}$ values in the city exceeded 500 µg m^{-3} on no less than six days during the month of December, prompting two official air pollution 'red alerts' to be issued (Xue et al., 2016). Close examination of the haze events demonstrate that they occur in cycles of a few days and generally coincide with winds blowing from the more polluted regions south of the city (Guo et al., 2014;Wu et al., 2007). Particulate matter concentrations are observed to drop significantly when the winds change to a northerly direction, bringing cleaner air into the city, which is when NPF events generally occur (Guo et al., 2014).

The earliest study of NPF using a TSI scanning mobility particle sizer (SMPS) in Beijing was carried out by Wehner et al. (2004). They observed NPF on 25 out of 45 days of measurement with PNCs exceeding 10^5 cm^{-3}. Subsequent studies using the SMPS were carried out by Wu et al. (2007) who showed that NPFs were observed on 50%, 20%, 35% and 45% of days during the spring, summer, fall and winter seasons, respectively. Yue et al. (2010) investigated 12 NPF events and showed that sulphuric acid and ammonia accounted for about 45% of the growth rate, with the balance being due to organic species. Guo et al. (2014) conducted a detailed analysis over a two-month period during the fall of 2013 and showed that NPF events occurred in a clear periodic cycle of about 4-7 days coinciding with northerly winds bringing cleaner air into the city. The average $PM_{2.5}$ values when the wind was from the north and when it was from the south were 35 and 114 µg m^{-3}, respectively. The average $PM_{2.5}$ (and PNC) values during and outside the NPF periods were less than 50 µg m^{-3} (greater than 2 x 10^5 cm^{-3}) and several hundred µg m^{-3} (5 x 10^4 cm^{-3}), respectively. Pollution also originates from within the city – from motor vehicle emissions and industrial sources. In general, airborne gaseous pollutants in Beijing and other urban regions in China are mainly volatile organic compounds (VOC) and oxides of nitrogen (NO_x) from local transportation and sulphur dioxide (SO_2) from regional industrial sources (Wang et al., 2009;Yue et al., 2010). However, Guo et al. (2014) showed that the nucleation and growth processes occurred on a regional scale, over several hundred km, with the effect of local sources such as motor vehicle emissions being insignificant. A good summary of the studies conducted since 2004 in Beijing may be found in Zhibin et al. (2013) and Kulmama et al. (2016).

Atmos. Chem. Phys. Discuss., doi:10.5194/acp-2017-156, 2017
Manuscript under review for journal Atmos. Chem. Phys.
Discussion started: 1 March 2017

All these previous studies in Beijing have been carried out using the SMPS. The SMPS is a good tool to determine the PNC and size distribution down to a minimum particle size of about 3 nm, although the efficiency of detection falls off below about 10 nm. Thus, an event where aerosols in the size range 3-10 nm emitted on-site as primary particles or entrained from a distant location that continue to grow to larger sizes may be mistaken for particle formation at that monitoring site. The SMPS is also not able to identify the exact time period during which particle formation occurs. An instrument that can detect particles at smaller sizes is the neutral cluster and air ion spectrometer (NAIS) from Airel Ltd. The NAIS is specifically designed to monitor particle formation as it can detect particles down to a size of 0.8 nm (Manninen et al., 2016;Manninen et al., 2009;Mirme et al., 2007). In this paper, we present the first results of using a NAIS in Beijing over the course of three months, two months with intense haze and very few NPF events, and the other including several days with NPF. We will investigate the characteristics of the NPF events and the conditions that gave rise to them. As the measurements included the sizes at which particles formed, the results provide more reliable information of such parameters as the starting times, growth rates and formation rates of particles than has been possible in the past.

2. Methods

2.1 Instrumentation

The NAIS is an improved version of the air ion spectrometer (AIS) which was developed by Airel Ltd (Mirme et al., 2007). In both instruments, the sample air is split equally into each of two separate cylindrical spectrometer columns, one of each polarity. At the inlet to each column, a unipolar corona wire diffusion charger of the same polarity as the central electrode in the column brings the particles to an equilibrium charge distribution. They are then classified by a differential mobility analyser where the outer electrodes consist of 21 insulated sections or rings, each with its own electrometer. The charged particles in the air flow are repelled by the central electrode which has a tapered cross-section and collected by the rings. The electric field between the central electrode and the rings is fixed by the voltage on the inner electrode and the gap between the inner and outer electrodes so that only particles in a given mobility range may be collected by each ring. In this way, the instrument can separate particles into 21 mobility or size bins. A refinement in the NAIS over the AIS is that it uses controlled charging to measure the concentration of charged particles in addition to the total PNC in each size range. This is done by switching the voltage off on the corona charger during one part of the measurement cycle. Thus, the NAIS can measure both charged and neutral particles separately. The mobility range of the instrument is 3.16-0.001 $cm^2 V^{-1} s^{-1}$ which corresponds to a mobility diameter range of 0.8-42 nm. A good description of the detailed operation of the NAIS may be found in Manninen et al. (2016). In this study, we set the NAIS to a measurement cycle of 5 min consisting of 2 min each for charged and neutral particles with an offset period of 1 min. Thus, a PNC and charged particle concentration reading were obtained in real time once every 5 min.

The larger size PNC was monitored with an SMPS. The instrument was set to scan up and retrace times of 120 and 15 s respectively. The aerosol and sheath flow rates were 0.3 and 3.0 lpm, respectively. Size distributions were determined in 107 bins in the size range 14 to 673 nm. A complete size distribution record was obtained every 5 min. $PM_{2.5}$ concentrations were monitored with a tapered element oscillating monitor (TEOM) and recorded as hourly average values.

2.2 Study Design

The NAIS and SMPS were set up within a room on the roof of the Chinese Research in Atmospheric and Environmental Sciences (CRAES) Building in Beiyuan, Beijing, on the 28 October 2015 and monitoring was conducted continuously until 31 January 2016. This comprised 96 days including several episodes of very high pollution or haze days when the $PM_{2.5}$ in Beijing exceeded 100-200 µg m^{-3}. Owing to the high PM content in the air, the instrument experienced some problems on 9 days during which data was lost. Air was sampled through a straight steel pipe of diameter 4 cm protruding vertically through the roof of the building. Meteorological parameters, including the wind speed, wind direction, air temperature and relative humidity were monitored and recorded hourly over the course of the study period.

2.2 Analysis

2.2.1 Identification of NPF events

The NAIS provided spectragrams showing the neutral and charged particle number size distributions in real time with the concentrations shown in colour contours. The neutral and charged PNCs were also provided in real time at 5 min intervals. NPF events were identified using the method proposed by Zhang et al. (2004). We calculated the rate of change of PNC, dN/dt, where N is the number of particles in the size range 1.8 -10.0 nm. Events with N > 10,000 cm^{-3} for at least 1 hour and dN/dt >15,000 $cm^{-3}h^{-1}$ were classified as NPF events. These events generally exhibited a 'banana shape' in the spectragrams. A day on which there was at least one NPF event as defined above was termed an "NPF day". A day where the above criteria were not fulfilled were classified as a "non-event" day. NPF events are characterised by sharp increases in the intermediate size range. The starting times of an event was determined by using the time of sudden increase in PNC in the size range 1.8 – 10.0 nm.

2.2.2 Condensation sink (CS) and coagulation sink (CoagS)

The condensation sink of particles is defined as (Dal Maso et al., 2002;Dal Maso et al., 2005;Kulmala et al., 2012;Lehtinen et al., 2003;Salma et al., 2011)

$$CS = 2\,\pi\,D\,\sum_i \beta_m\,(d_{p,i})d_{p,i}N_i \qquad (1)$$

where D is the diffusion coefficient of the condensing vapour and β_m is the transition correction factor for mass flux. d_{pi} and N_i are the diameter and the number concentration of particles in the size bin i respectively. The unit of CS is s^{-1}.

Assuming that the main condensing vapour is sulphuric acid, we estimated the diffusion coefficient for condensing vapour using the expression

$$D = 5.0032 * 10^{-6} + 1.04 * 10^{-8} T + 1.64 * 10^{-11} T^2 - 1.566 * 10^{-14} T^3 \qquad (2)$$

where D has the units of $m^2\ s^{-1}$ and where the temperature T is in Kelvin (Jeong, 2009).

The transition correction factor, β_m, was calculated using the Fuchs-Sutugin expression (Fuchs and Sutugin, 1971)

$$\beta_m = \frac{Kn + 1}{1 + (\frac{4}{3\alpha} + 0.337)Kn + (\frac{4}{3\alpha})Kn^2} \qquad (3)$$

where

$$Kn = \frac{2\lambda}{d_p} \quad \text{and} \quad 0 \leq \alpha \leq 1 .$$

Here, Kn, the Knudsen number, describes the nature of the suspending vapour relative to the particle, λ is the mean free path of a suspending vapour molecule and d_p is the diameter of the particle (Seinfeld and Pandis, 2006). The mass accommodation coefficient (sticking coefficient) α describes the probability of a vapour molecule sticking to the surface of a particle during vapour-particle interactions (Seinfeld and Pandis, 2006). In this study, we assumed $\alpha = 1$.

The relationship between the condensation sink and coagulation sink is given by Lehtinen et al. (2007) as

Atmos. Chem. Phys. Discuss., doi:10.5194/acp-2017-156, 2017
Manuscript under review for journal Atmos. Chem. Phys.
Discussion started: 1 March 2017

$$CoagS_{d_p} = CS.\left(\frac{d_p}{0.71}\right)^m \quad (4)$$

where the exponent m varies in the range -1.75 to -1.5 with a mean value -1.7 and the value 0.71 is the diameter of a hydrated sulphuric acid molecule. The unit of CoagS is s^{-1}.

In order to calculate the CS, we used the PNC obtained from the SMPS in the 107 size bins. We calculated *D* using equation (2) at temperature T = 303 K. The values used for the exponent m was -1.7 (Dal Maso et al., 2008) and λ =108 nm (Massman, 1998).

2.2.3 Particle formation rate

Particle formation or nucleation occurs from thermodynamically stable clusters in the size range 1.0-2.0 nm (Kulmala et al., 2007). The formation rate may be estimated from the number of particles in the smallest size bin, usually 2-3 nm in the NAIS.

The formation rate of particles is defined as

$$J_{d_p} = \frac{dN_{d_p}}{dt} + CoagS_{d_p}.N_{d_p} + \left(\frac{GR}{\Delta d_p}\right)N_{d_p} \quad (5)$$

where N_{dp} is the number concentration of particles in the size range d_p and (d_p + Δd_p) respectively (Kulmala et al., 2012). In this study, we used the values d_p = 2 nm and Δd_p = 1 nm, corresponding to the size range 2-3 nm. $CoagS_{dp}$ represents the loss of the particles due to coagulation and *GR* is the growth rate of particles. The unit of formation rate is cm^{-3} s^{-1}.

Atmos. Chem. Phys. Discuss., doi:10.5194/acp-2017-156, 2017
Manuscript under review for journal Atmos. Chem. Phys.
Discussion started: 1 March 2017

Atmospheric Chemistry and Physics Discussions

2.2.4 Particle growth rate (GR)

During an NPF event, the growth rate of particles was defined by Kulmala et al. (2012) as

$$GR = \frac{dd_p}{dt} = \frac{d_{p2} - d_{p1}}{t_2 - t_1} \quad (6)$$

where dp_2 and dp_1 are the diameters of particles at times t_2 and t_1, respectively. This was calculated by the maximum concentration method as described in Kulmala et al. (2012) by examining the time of maximum PNC at each particle size during an NPF event. First, we exported the number concentrations of particles obtained from the NAIS in 15 bins in the size range 1.8 – 42.0 nm. Next, we selected the time of maximum concentrations during each NPF event for each particle size bin. Finally, we calculated the growth rate using the slope of the best-fitted line on the graph of median diameter of particle in each size bin vs. the time of maximum concentration. The unit of GR is nm h^{-1}.

3. Results and Discussion

3.1 Distribution of NPF events

During the entire period of measurement, the NAIS yielded 87 complete days of data, the remaining 9 days being affected by instrument faults, generally due to power fluctuations. November and December 2015 were particularly prone to high pollution events in Beijing. The daily average $PM_{2.5}$ concentration exceeded the recommended maximum of 50 µg m^{-3} in Beijing on 47 days during this two-month period. The maximum daily average was 448 µg m^{-3} and this occurred on 1st December. Owing to the high condensation sink on polluted days, there were relatively few NPF days during these two months. There was a relative improvement of air quality after 4th January and this lasted until 31st January - the end of the monitoring period, during which time, the daily average exceeded 100 µg m^{-3} on only four days. Enhanced $PM_{2.5}$

Atmos. Chem. Phys. Discuss., doi:10.5194/acp-2017-156, 2017
Manuscript under review for journal Atmos. Chem. Phys.
Discussion started: 1 March 2017

Atmospheric Chemistry and Physics Discussions

concentrations (> 50 µg m^{-3}) were observed on 15 days in January. These days occurred in groups and we could identify five such distinct periods during January. No NPF events were observed during these 15 days; however, several NPF events were observed on the other days during the intervening periods. A summary of the observational days, together with the number of days on which data were available and NPF events were observed, are shown in Table 1. Column 3 shows the numbers of days on which complete 24-hour data were obtained. We note that, during the 56 such days between 27th October and 31st December, NPF events were observed on just 10 days, whereas during the 31 days in January 2016, NPF events took place on 16 days. The near equal division between NPF days and no-NPF days in January provided an ideal data set to compare the parameters and conditions on these two types of days. The difference between November/December and January had a clear dependence on the $PM_{2.5}$ concentrations. Figure 1 gives a summary of the days on which NPF events were observed.

3.2 Relationship between NPF events and $PM_{2.5}$ concentration

In Fig 2, we take a closer look at the January data, together with the respective mean daily $PM_{2.5}$ concentrations. It is apparent that there were five distinct groups of NPF days in January. These are labelled in 2(b). In the NAIS spectragram, shown in 2(a), the 16 NPF events are clearly observed with the characteristic 'banana' shapes compressed into near-vertical bands extending up from the smallest sizes. The five groups from left to right consist of 5, 3, 2, 5 and 1 NPF events, respectively (Figs 2(a and b)). These groups are separated by time periods when no NPFs were observed. The $PM_{2.5}$ values are clearly lower on NPF days than on the other days with mean daily values of 18 µg m^{-3} and 120 µg m^{-3}, respectively. A Student's t-test showed that the difference in mean daily $PM_{2.5}$ values between NPF days and the other days was statistically significant at the confidence level of 95%. Figure 2(c) shows the corresponding mean daily PNC. While the PNC within each group showed a greater fluctuation than the $PM_{2.5}$, the PNC on NPF days was significantly higher than on non-NPF days. Therefore, although the PM is higher on

Atmos. Chem. Phys. Discuss., doi:10.5194/acp-2017-156, 2017
Manuscript under review for journal Atmos. Chem. Phys.
Discussion started: 1 March 2017

Atmospheric Chemistry and Physics Discussions

haze days than on NPF days, the t-tests again showed that the PNC was significantly lower on haze days than on NPF days. This is explicable in terms of the particle size. Particles are significantly larger on haze days than on clean days when NPF events are likely to occur.

In Fig 3, we plot the daily mean PNC against the daily mean $PM_{2.5}$ for the 31 days in January. The days with NPF and the days with no NPF events clearly fall into two distinct groups according to the daily mean $PM_{2.5}$ values. No NPF events were observed on a day when the mean $PM_{2.5}$ value exceeded 43 µg m^{-3}. There is some minor overlap in the PNC values on the two types of days but this is primarily because they are daily averages. When we consider the average PNC values during the NPF events alone, a t-test showed that they are significantly higher than at other days and times. However, we do see that, on haze days, the daily average PNC does not exceed 8.5×10^4 cm^{-3}.

3.3 Relationship between NPF events and wind direction

Previous studies have shown that the wind direction played an important role in determining the $PM_{2.5}$ concentration in Beijing (Guo et al., 2014). Again, we look at the month of January, as it provided an almost equal number of NPF days and non-NPF days and was, therefore, ideal to compare the wind direction on the two types of days. Figure 4 shows the wind direction roses for both NPF days and non-NPF days during January. The frequencies are given as percentages of time when the wind was from a given direction. There is a clear difference between the two sets of days with a strong correlation between the NPF days and the wind direction. NPF events clearly occurred on days when the wind direction was predominantly from the NW, while it was more equally distributed with a greater likelihood of arriving from the S and E during the haze days when there were no NPF events. The frequencies in the sector between NW (315°) and N (0°) on NPF days and non-NPF days were 68 % and 11 %, respectively. Air from the north of Beijing is usually cleaner than that from the more industrialized south of the city (Guo et al., 2014). Clean periods are characterised

Atmos. Chem. Phys. Discuss., doi:10.5194/acp-2017-156, 2017
Manuscript under review for journal Atmos. Chem. Phys.
Discussion started: 1 March 2017

by decreased condensation sinks that promote NPF. Winds from the south bring a copious supply of freshly available gaseous precursors that should give rise to particle formation. However, the absence of NPF events during these times suggests that the wind is also carrying a large supply of particles that reduce the gaseous supersaturations required for particle formation. Thus, the observed haze events are more likely to be due to particles carried by the wind into the city or being prevented from escaping due to temperature inversions in the atmosphere.

3.4 Charged particles and clusters

Next, we look at the behaviour of charged clusters and charged particles, with particular attention to NPF events and haze events. In order to compare and contrast the characteristics of these particles, we selected a period of four days, comprising two haze days that were immediately followed by two NPF days. Figure 5 shows the time series of the concentration of total and charged particles (a) and clusters (b) observed over this four-day period from November 30 to December 3. In Fig 5(a), the upper curve represents the total PNC while the lower curve gives the charged PNC. The difference between the two curves gives the neutral PNC. This is similar for the cluster concentrations in Fig 5(b). The conditions during the two types of events could be compared during this period as intense haze was observed on the first two days (Nov 30 and Dec 1) while, following a change of wind direction near midnight on the 1 December, two strong NPF events took place on the next two days (Dec 2 and 3). In general, the neutral cluster concentration exceeded the cluster ion concentration by about two orders of magnitude, with this ratio being somewhat greater when there was no particle formation. Large pools of neutral clusters were always observed to be present in previous studies in the boreal forests of Hyytiala, Finland (Kulmala et al., 2007) and in the urban environment of Brisbane, Australia (Jayaratne et al., 2016). Here, we can confirm the same observation in the more polluted Beijing atmosphere. The total cluster concentration showed a significant decrease, by almost an order of magnitude, as we passed from the first two days to the two NPF days. We attribute this to two phenomena - the attachment of clusters to existing particles and the conversion

Atmos. Chem. Phys. Discuss., doi:10.5194/acp-2017-156, 2017
Manuscript under review for journal Atmos. Chem. Phys.
Discussion started: 1 March 2017

of clusters to new particles. We also see that less than 10% of the particles were charged, both during NPF days and when there were no NPF events.

A summary of the neutral and charged PNC and cluster concentrations during the various stages over the entire period of observation are presented in Table 2. Also shown are the percentage numbers of all particles that were found to be charged. NPF events and NPF days are defined in section 2.2.1. A haze day was defined as a day when the 24-hour average $PM_{2.5}$ concentration exceeded 75 µg m^{-3} - the national air quality standard in China. A day that met neither of these criteria was defined as a 'normal day'. Thus, by our ad-hoc definition, a normal day had a daily average $PM_{2.5}$ concentration in the range 43-75 µg m^{-3}, since no NPF events were observed on days when the average $PM_{2.5}$ concentration was greater than 43 µg m^{-3}. The duration of the various events affected the daily values while the conditions during the events affected their peak number concentrations. This introduced an inherent uncertainty of up to 20% in the values shown in the table.

We note that only a very small percentage of clusters, less than 1%, are charged under all conditions. On a normal day, around 15% of the particles larger than 2 nm are charged. The fraction that is charged decreases significantly during an NPF event. This is consistent with our observations in Brisbane (Jayaratne et al., 2016) and may be attributed to the rapid increase in particle number and the associated coagulation. On the other hand, during a haze event, the percentage of particles charged increases to a value between 20% and 30%. These observations are consistent with the PNC and particle sizes and the equilibrium distribution of charge on particles. NPF are characterised by large numbers of small particles while the SMPS and TEOM show that haze events comprise much larger particles. The amount of charge that a particle can hold and the fraction of particles that are charged in equilibrium both increase with particle size, so it is not unexpected to find that a larger percentage of particles are charged during the haze events.

3.5 Particle formation times

All except one of the 26 NPF events during the period of observation began between 7:30 am and 10:00 am. The mean time was 8:45 am. This result is in agreement with Wu et al. (2007) who, using an SMPS, reported that NPF events during clean air periods in November, December and January generally started between 7:00 am and 10:00 am. Figure 6 shows the temporal distribution of the start times of the NPF events, classified into 30 minute bins. The most likely time for an NPF event to begin was between 8:00 and 8:30 am. This time coincides with the morning rush hour traffic when the production rate of gaseous precursors is generally at a maximum. Sunrise in Beijing in December/January is at about 7.30 am.

Figure 7 shows the NAIS spectragram of the strong NPF event that occurred on 29th October 2015. The spectragram shows a clear banana profile which levels off at about 20 nm. The PNC in this event was relatively high, exceeding 1.6 x 10^5 cm^{-3} near 11:00 am. The $PM_{2.5}$ concentration remained between 12 and 16 µg m^{-3} right through this event. The markers shown on this figure are the median sizes of particles at each time. In the spectragram, the transition time from clusters to particles, at around 2 nm, is very sharp and we can conclude that particle formation began at around 09:00 h. However, previous studies in Beijing have not been able to measure particles smaller than 3 nm. In Fig 7, if we truncate the lower particle size margin to 3 nm, the starting time of the NPF event appears later than it actually is, approximately at 9:30 am. In other NPF spectragrams, we see this difference being as much as 1.0 to 1.5 h depending on the initial growth rate. Thus, we conclude that the starting times that we have derived (Fig 6) are more accurate than has been obtained in the past. This will also affect the estimated growth rates of particles during NPF events as we shall show in the next section.

3.6 Condensation and coagulation sinks

The condensation and coagulation sinks were calculated during NPF events assuming the growth to be due to sulfuric acid and using the SMPS data and the equations given in the methods section. The mean value of the condensation sink was $5x10^{-3}$ s^{-1}. This value is somewhat smaller than that reported by Wu et al. (2007) ($1.4x10^{-2}$ s^{-1}) and Wu et al. (2011) ($1x10^{-2}$ s^{-1}) but within the range of 0 – $5x10^{-2}$ s^{-1} reported in all NPF events between 2004 to 2008 in Beijing by Zhibin et al. (2013). The mean value of our coagulation sink for 2 nm particles during an NPF event was $9x10^{-4}$ s^{-1}. Previous studies in Beijing have not been able to determine this value at 2 nm. The values reported for 3, 5 and 10 nm for NPF events in Beijing by Wu et al. (2011) are $9.9x10^{-4}$ s^{-1}, $4.3x10^{-4}$ s^{-1} and $1.4x10^{-4}$ s^{-1}, respectively. The value at 3 nm is close to our value at 2 nm.

3.7 Particle formation rate

Using the values of the condensation and coagulation sinks in equation 5, we calculated the formation rate of particles in the smallest particle size bin 2-3 nm where the rate of increase of particles ranged from about $5.0x10^{3}$ to $1.5x10^{4}$ cm^{-3} h^{-1}. The resulting formation rates varied between 10 and 36 cm^{-3} s^{-1}, with a mean of 23 cm^{-3} s^{-1}. Previous estimates in Beijing did not have the benefit of the information in the 2-3 nm size bin. Wu et al. (2007) calculated the formation rate in the wider size bin of 3-10 nm and arrived at a value in the range 3.3-81.4 cm^{-3} s^{-1} with a mean of 22.3 cm^{-3} s^{-1}. Yue et al. (2010) studied 12 NPF events in Beijing and derived a formation rate in the range 2-13 cm^{-3} s^{-1} and showed that the formation rate was directly proportional to the sulfuric acid concentration. They did not specify the size range used in this calculation but the smallest detectable particle size of the instrument used was 3 nm.

Atmos. Chem. Phys. Discuss., doi:10.5194/acp-2017-156, 2017
Manuscript under review for journal Atmos. Chem. Phys.
Discussion started: 1 March 2017

3.8 Particle growth rate

In the NPF event shown in Fig 7, the particle growth rate soon after formation is about 9 nm h^{-1}. The average growth rate during the entire event (between 9:00 and 11:00 am) estimated from equation 6 was 4.8 nm h^{-1}. Although the PNC reached very high values, the particles did not grow much larger than about 30 nm, suggesting that the high condensation sink was restricting the precursor gas concentration in the atmosphere. The growth rate of all the NPFs observed ranged from 0.5 to 9.0 nm h^{-1} with a mean value of 3.5 nm h^{-1}. Previous estimates of the growth rate during NPF using the SMPS have yielded mean values of 1.0 nm h^{-1} (Wehner et al., 2004) and 1.8 nm h^{-1} (Wu et al., 2007)., 2007). Zhibin et al. (2013) determined the growth rates of a number of NPFs in Beijing over a 4-year period and reported a range of 0.1 to 10 nm h^{-1} with a mean of 3.0 nm h^{-1} which is in close agreement with our value.

4. Summary and Conclusions

We monitored charged and neutral PNC over a continuous three-month period for the first time in Beijing. The results showed 26 NPF events. No NPF were observed when the daily mean $PM_{2.5}$ concentration exceeded 43 µg m^{-3}.

A summary of the main parameters determined are shown in Table 3.

This is the first study of NPF in the particle size range below 3 nm in Beijing. This enables the derivation of more relevant and accurate estimates of parameters, such as the times of formation and growth and formation rates, than has been possible before.

The results show the following features of NPF events in Beijing:

- NPF events occur during clean air episodes when the wind direction is from the north of the city.
- We have provided the first temporal distribution chart of NPF events in Beijing which shows that all but one of the 26 events began between 7:30 and 10:00 am.
- The main characteristics of the particles in the NPF events are presented in Table 3.
- In general, less than 10% of particles were charged and less than 1% of the clusters were charged.
- The fraction of particles that are charged was normally about 15%. This fraction increased to 20-30% during haze events and decreased to below 10% during NPF events.

Acknowledgements

This project was supported by the Australia-China Centre for Air Quality Science and Management.

Atmos. Chem. Phys. Discuss., doi:10.5194/acp-2017-156, 2017
Manuscript under review for journal Atmos. Chem. Phys.
Discussion started: 1 March 2017

Atmospheric Chemistry and Physics Discussions

References

Curtius, J.: Nucleation of atmospheric aerosol particles, Comptes Rendus Physique, 7, 1027-1045, 2006.

Dal Maso, M., Kulmala, M., Lehtinen, K., Mäkelä, J., Aalto, P., and O'Dowd, C.: Condensation and coagulation sinks and formation of nucleation mode particles in coastal and boreal forest boundary layers, Journal of Geophysical Research: Atmospheres, 107, 2002.

Dal Maso, M., Kulmala, M., Riipinen, I., Wagner, R., Hussein, T., Aalto, P. P., and Lehtinen, K. E.: Formation and growth of fresh atmospheric aerosols: eight years of aerosol size distribution data from SMEAR II, Hyytiala, Finland, Boreal Environment Research, 10, 323, 2005.

Dal Maso, M., Hyvärinen, A., Komppula, M., Tunved, P., KERMINEN, V., Lihavainen, H., Viisanen, Y., HANSSON, H. C., and Kulmala, M.: Annual and interannual variation in boreal forest aerosol particle number and volume concentration and their connection to particle formation, Tellus B, 60, 495-508, 2008.

Fuchs, N., and Sutugin, A.: High-dispersed aerosols, Topics in Current Aerosol Research GM Hidy, JR Brock, 1–60, in, Pergamon, New York, 1971.

Guo, S., Hu, M., Zamora, M. L., Peng, J., Shang, D., Zheng, J., Du, Z., Wu, Z., Shao, M., and Zeng, L.: Elucidating severe urban haze formation in China, Proceedings of the National Academy of Sciences, 111, 17373-17378, 2014.

Huang, R.-J., Zhang, Y., Bozzetti, C., Ho, K.-F., Cao, J.-J., Han, Y., Daellenbach, K. R., Slowik, J. G., Platt, S. M., and Canonaco, F.: High secondary aerosol contribution to particulate pollution during haze events in China, Nature, 514, 218-222, 2014.

Jayaratne, E., Clifford, S., and Morawska, L.: Atmospheric Visibility and PM10 as Indicators of New Particle Formation in an Urban Environment, Environmental science & technology, 49, 12751-12757, 2015.

Jayaratne, E. R., Ling, X., and Morawska, L.: Charging State of Aerosols during Particle Formation Events in an Urban Environment and Its Implications for Ion-Induced Nucleation, Aerosol and Air Quality Research, 16, 348-360, 2016.

Jeong, K.: Condensation of water vapor and sulfuric acid in boiler flue gas, ProQuest, 2009.

Kulmala, M., Vehkamaki, H., Petaja, T., Dal Maso, M., Lauri, A., Kerminen, V., Birmilli, W., and McMurry, P.: Formation and Growth Rates of Ultrafine Atmospheric Particles: A Review of Observations, Journal of Aerosol Science, 35, 143-176, 2004.

Kulmala, M., Petäjä, T., Mönkkönen, P., Koponen, I., Maso, M. D., Aalto, P., Lehtinen, K., and Kerminen, V.-M.: On the growth of nucleation mode particles: source rates of condensable vapor in polluted and clean environments, Atmospheric Chemistry and Physics, 5, 409-416, 2005.

Kulmala, M., Riipinen, I., Sipilä, M., Manninen, H. E., Petäjä, T., Junninen, H., Dal Maso, M., Mordas, G., Mirme, A., and Vana, M.: Toward direct measurement of atmospheric nucleation, Science, 318, 89-92, 2007.

Kulmala, M., Petäjä, T., Nieminen, T., Sipilä, M., Manninen, H. E., Lehtipalo, K., Dal Maso, M., Aalto, P. P., Junninen, H., and Paasonen, P.: Measurement of the nucleation of atmospheric aerosol particles, Nature protocols, 7, 1651-1667, 2012.

Kulmama, M., Petäjä, T., Kerminen, V.-M., Kujansuu, J., Ruuskanen, T., Ding, A., Nie, W., Hu, M., Wang, Z., and Wu, Z.: On secondary new particle formation in China, Frontiers of Environmental Science & Engineering, 10, 1-10, 2016.

Lehtinen, K. E., Korhonen, H., Maso, M., and Kulmala, M.: On the concept of condensation sink diameter, Boreal environment research, 8, 405-412, 2003.

Lehtinen, K. E., Dal Maso, M., Kulmala, M., and Kerminen, V.-M.: Estimating nucleation rates from apparent particle formation rates and vice versa: Revised formulation of the Kerminen–Kulmala equation, Journal of Aerosol Science, 38, 988-994, 2007.

Manninen, H. E., Petaja, T., Asmi, E., Ripinen, I., Nieminen, T., Mikkila, J., Horrak, U., Mirme, A., Mirme, S., Laakso, L., Kerminen, V., and Kulmala, M.: Long-term field measurements of charged and

Atmos. Chem. Phys. Discuss., doi:10.5194/acp-2017-156, 2017
Manuscript under review for journal Atmos. Chem. Phys.
Discussion started: 1 March 2017

Atmospheric Chemistry and Physics Discussions
Open Access
EGU

neutral clusters using Neutral cluster and Air Ion Spectrometer (NAIS), Boreal Environment Research, 14, 591-605, 2009.

Manninen, H. E., Mirme, S., Mirme, A., Petäjä, T., and Kulmala, M.: How to reliably detect molecular clusters and nucleation mode particles with Neutral cluster and Air Ion Spectrometer (NAIS), Atmos. Meas. Tech. Discuss, 2016.

Massman, W.: A review of the molecular diffusivities of H_2O, CO_2, CH_4, CO, O_3, SO_2, NH_3, N_2O, NO, and NO_2 in air, O_2 and N_2 near STP, Atmospheric Environment, 32, 1111-1127, 1998.

Mirme, A., Tamm, E., Mordas, G., Vana, M., Uin, J., Mirme, S., Bernotas, T., Laakso, L., Hirsikko, A., and Kulmala, M.: A wide-range multi-channel Air Ion Spectrometer, Boreal Environmental Research, 12, 247-264, 2007.

Salma, I., Borsós, T., Weidinger, T., Aalto, P., Hussein, T., Dal Maso, M., and Kulmala, M.: Production, growth and properties of ultrafine atmospheric aerosol particles in an urban environment, Atmos. Chem. Phys, 11, 1339-1353, 2011.

Seinfeld, J. H., and Pandis, S. N.: Atmospheric chemistry and physics. Hoboken, NJ: Wiley, 2006.

Wang, M., Zhu, T., Zheng, J., Zhang, R., Zhang, S., Xie, X., Han, Y., and Li, Y.: Use of a mobile laboratory to evaluate changes in on-road air pollutants during the Beijing 2008 Summer Olympics, Atmospheric Chemistry and Physics, 9, 8247-8263, 2009.

Wehner, B., Wiedensohler, A., Tuch, T., Wu, Z., Hu, M., Slanina, J., and Kiang, C.: Variability of the aerosol number size distribution in Beijing, China: New particle formation, dust storms, and high continental background, Geophysical Research Letters, 31, 2004.

Wu, Z., Hu, M., Liu, S., Wehner, B., Bauer, S., Wiedensohler, A., Petäjä, T., Dal Maso, M., and Kulmala, M.: New particle formation in Beijing, China: Statistical analysis of a 1-year data set, Journal of Geophysical Research: Atmospheres, 112, 2007.

Wu, Z., Hu, M., Yue, D., Wehner, B., and Wiedensohler, A.: Evolution of particle number size distribution in an urban atmosphere during episodes of heavy pollution and new particle formation, Science China Earth Sciences, 54, 1772-1778, 2011.

Atmos. Chem. Phys. Discuss., doi:10.5194/acp-2017-156, 2017
Manuscript under review for journal Atmos. Chem. Phys.
Discussion started: 1 March 2017

Atmospheric Chemistry and Physics Discussions

Xiao, S., Wang, M., Yao, L., Kulmala, M., Zhou, B., Yang, X., Chen, J., Wang, D., Fu, Q., and Worsnop, D.: Strong atmospheric new particle formation in winter in urban Shanghai, China, Atmospheric Chemistry and Physics, 15, 1769-1781, 2015.

Xue, Y., Zhou, Z., Nie, T., Pan, T., Qi, J., Nie, L., Wang, Z., Li, Y., Li, X., and Tian, H.: Exploring the Severe Haze in Beijing During December, 2015: Pollution Process and Emissions Variation, Huan jing ke xue= Huanjing kexue/[bian ji, Zhongguo ke xue yuan huan jing ke xue wei yuan hui" Huan jing ke xue" bian ji wei yuan hui.], 37, 1593, 2016.

Yue, D., Hu, M., Zhang, R., Wang, Z., Zheng, J., Wu, Z., Wiedensohler, A., He, L., Huang, X., and Zhu, T.: The roles of sulfuric acid in new particle formation and growth in the mega-city of Beijing, Atmospheric Chemistry and Physics, 10, 4953-4960, 2010.

Zhang, Q., Stanier, C., Canagaratna, M., Jayne, J., Worsnop, D., Pandis, S., and Jiminez, J.: Insights into the Chemistry of New Particle Formation and Growth Events in Pittsburgh Based on Aerosol Mass Spectrometry, Environmental Science and Technology, 38, 4797-4809, 2004.

Zhang, R., Khalizov, A., Wang, L., Hu, M., and Xu, W.: Nucleation and growth of nanoparticles in the atmosphere, Chemical Reviews, 112, 1957-2011, 2011.

Zhibin, W., Min, H., Zhijun, W., and Dingli, Y.: Reasearch on the Formation Mechanisms of New Particles in the Atmosphere, Acta Chimica Sinica, 71, 519-527, 2013.

Atmos. Chem. Phys. Discuss., doi:10.5194/acp-2017-156, 2017
Manuscript under review for journal Atmos. Chem. Phys.
Discussion started: 1 March 2017

Figures

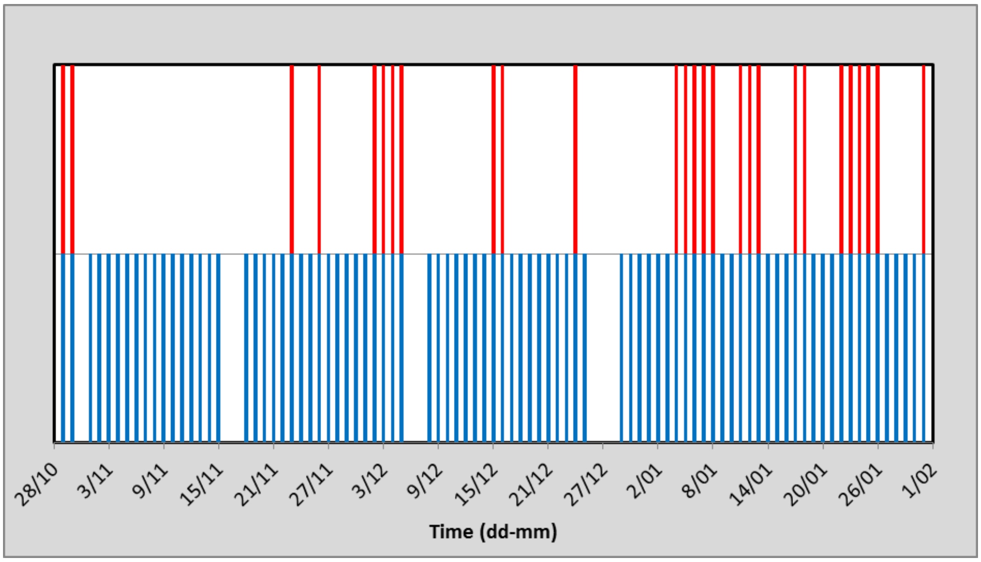

Figure 1: Summary of observational days (lower panel in blue) and days with NPF events (upper panel in red).

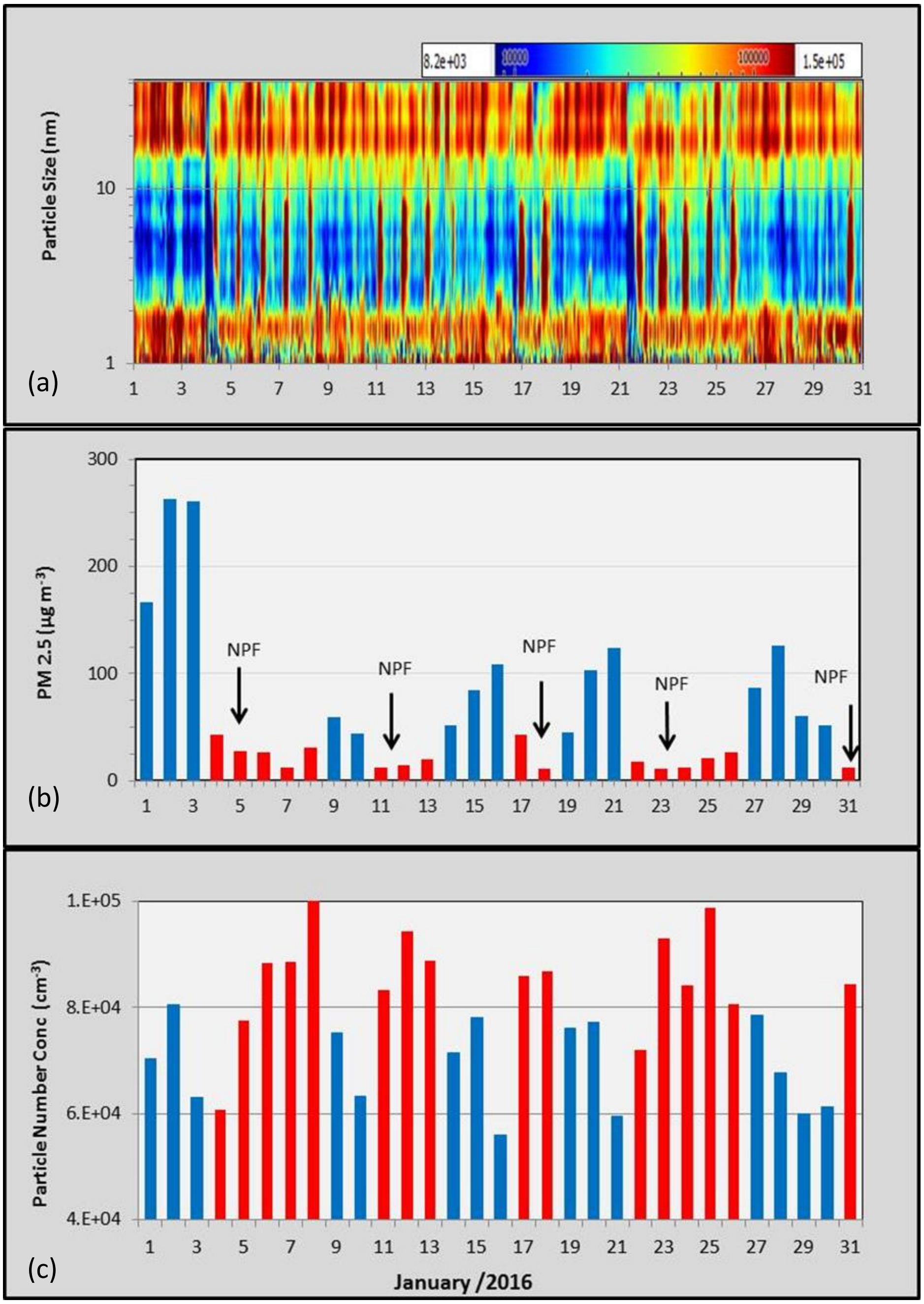

Figure 2: Daily values for January 2016: (a) NAIS Spectragram of PNC on a particle size–time diagram (b) mean $PM_{2.5}$ concentration from the TEOM and (c) mean PNC in the size range 1.8 – 42 nm from the NAIS. The red and blue bars represent the NPF and Non-NPF days, respectively.

Atmos. Chem. Phys. Discuss., doi:10.5194/acp-2017-156, 2017
Manuscript under review for journal Atmos. Chem. Phys.
Discussion started: 1 March 2017

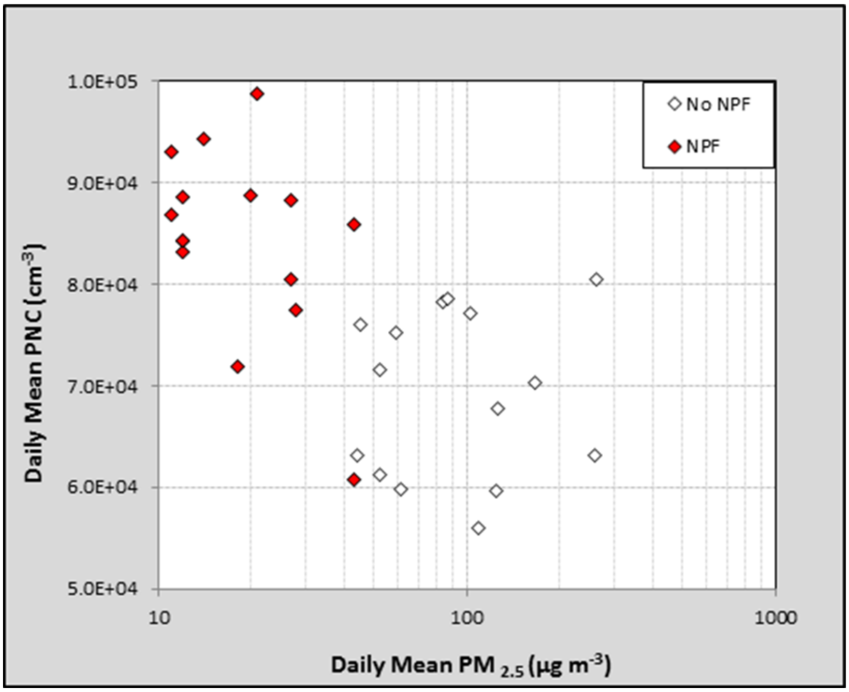

Figure 3: Daily mean PNC vs $PM_{2.5}$ for NPF days (filled markers) and no-NPF days (open markers) during January 2016.

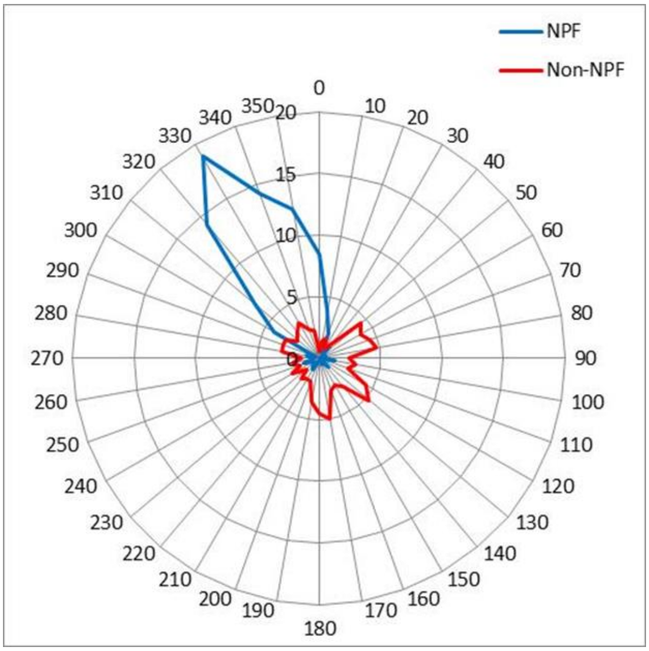

Figure 4: The wind direction rose for NPF days and non-NPF days during January. The radial scale indicates percentages of time.

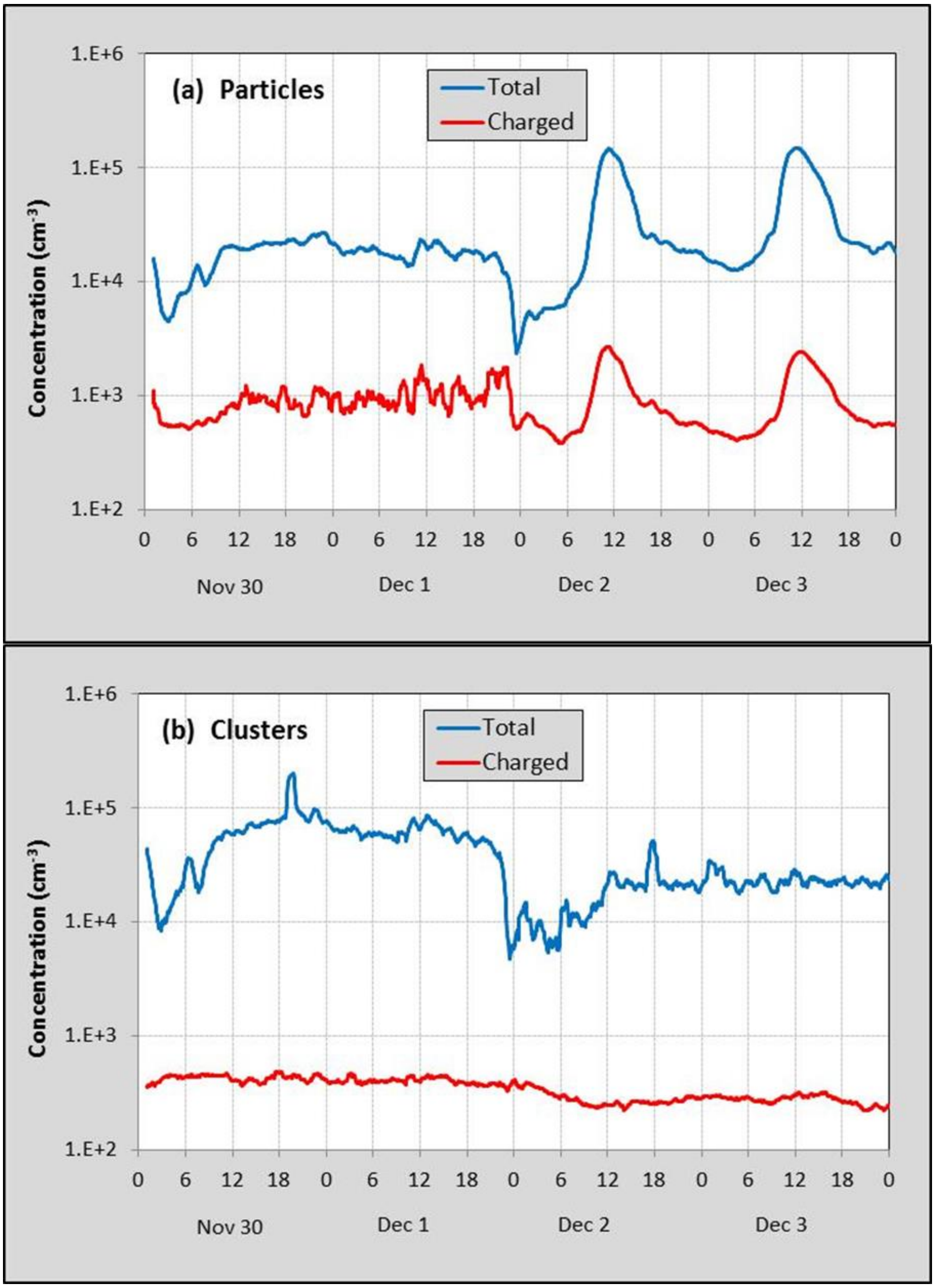

Figure 5: Time series of total and charged (a) particles and (b) clusters during the period 30 Nov to 3 Dec as measured by the NAIS. 30 Nov and 1 Dec were haze days while two NPF events occurred on 2 and 3 Dec.

Atmos. Chem. Phys. Discuss., doi:10.5194/acp-2017-156, 2017
Manuscript under review for journal Atmos. Chem. Phys.
Discussion started: 1 March 2017

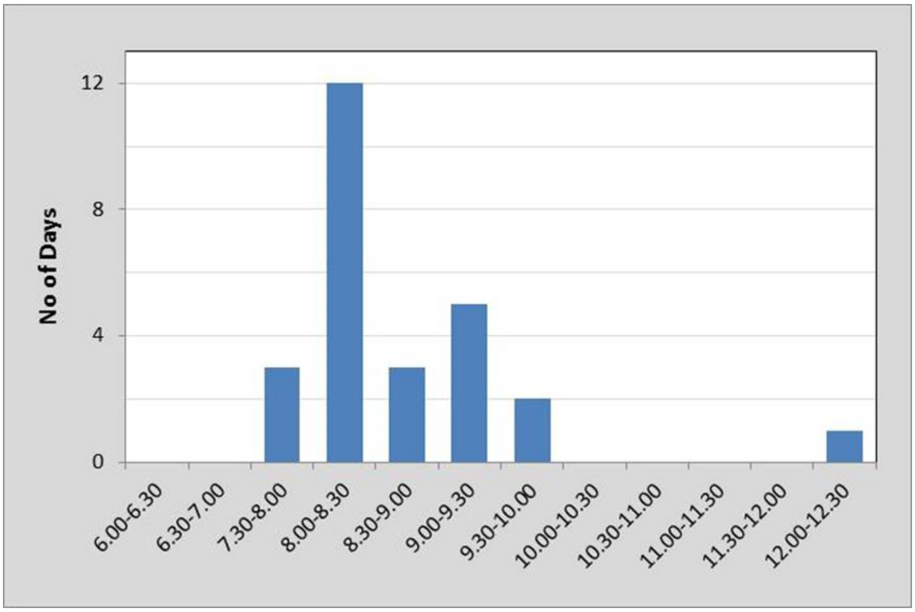

Figure 6: Distribution of the start times of the NPF events, classified into 30 min bins.

Atmos. Chem. Phys. Discuss., doi:10.5194/acp-2017-156, 2017
Manuscript under review for journal Atmos. Chem. Phys.
Discussion started: 1 March 2017

Atmospheric Chemistry and Physics Discussions
Open Access
EGU

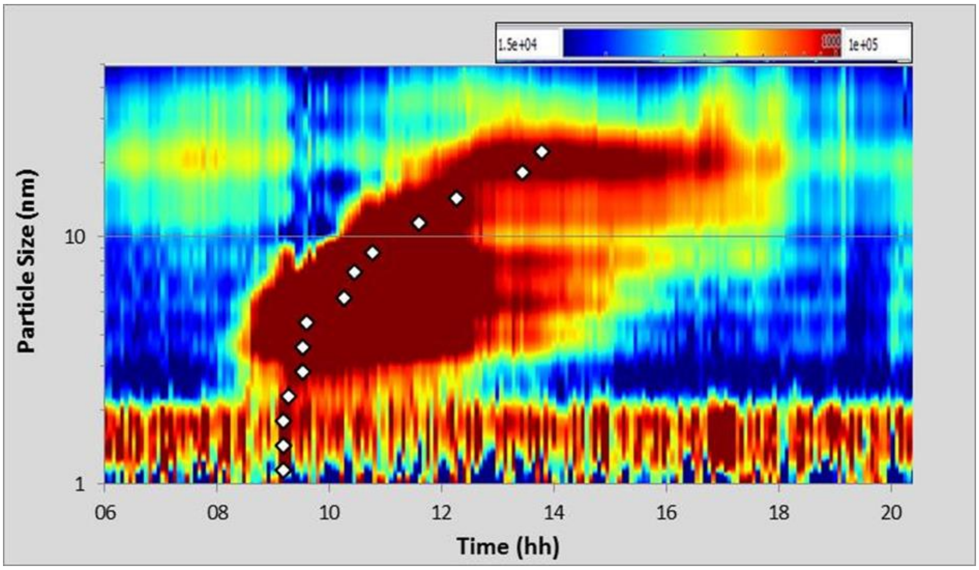

Figure 7: NAIS spectragram of the NPF event that occurred on 29th October. The clear banana shape indicates strong particle growth. The markers show the median particle size at each time.

Atmos. Chem. Phys. Discuss., doi:10.5194/acp-2017-156, 2017
Manuscript under review for journal Atmos. Chem. Phys.
Discussion started: 1 March 2017

Tables

Table 1: Summary of the observational days.

Month	Total Days	Data Available Days	NPF Days : dN/dt >15000 cm^{-3} h^{-1}
October (28-31)	4	2	2
November (1-30)	30	28	2
December (1-31)	31	26	6
January (1-31)	31	31	16
Total	96	87	26

Atmos. Chem. Phys. Discuss., doi:10.5194/acp-2017-156, 2017
Manuscript under review for journal Atmos. Chem. Phys.
Discussion started: 1 March 2017

Table 2: Mean and peak values of neutral and charged particle and cluster concentrations during the various types of days and events. The associated uncertainties in the values are up to 20%. The two % columns show the respective charged/total percentages.

	Particles (cm^{-3})			Clusters (cm^{-3})		
	Neutral ($x10^4$)	Charged ($x10^4$)	%	Neutral ($x10^4$)	Charged ($x10^2$)	%
Normal Days (mean)	5.9	1.0	15.0	3.1	1.5	0.5
NPF Days (mean)	8.0	0.9	10.1	2.6	1.4	0.5
NPF Events (peak)	23.7	1.4	5.4	4.9	3.3	0.7
Haze Days (mean)	5.0	2.0	28.2	3.8	2.4	0.6
Haze Events (peak)	12.3	3.1	20.0	9.9	4.8	0.5

Atmos. Chem. Phys. Discuss., doi:10.5194/acp-2017-156, 2017
Manuscript under review for journal Atmos. Chem. Phys.
Discussion started: 1 March 2017

Atmospheric Chemistry and Physics Discussions

641

642 Table 3: Summary of mean and range of parameters calculated for the NPF events observed.

Parameter	Mean	Range
Starting Time of NPF	8.45 am	7.30 am – 12.30 pm
Condensation sink (s^{-1})	5 x 10^{-3}	(2.1 – 8.9) x 10^{-3}
Coagulation sink (s^{-1})	9 x 10^{-4}	(3.6 -15.3) x 10^{-4}
Formation rate (J_2) (cm^{-3} s^{-1})	23	10 - 36
Growth rate (nm h^{-1})	3.5	0.5 - 9.0

643

644